Adhesion of cardiomyocytes on functionalized lipid bilayers

by L.G. van der Woerd

Faculty of Science and Technology
Biomedical Engineering

UNIVERSITY OF TWENTE.

July 22, 2021

Adhesion of cardiomyocytes on functionalized lipid bilayers

A bachelor thesis presented to obtain a BSc in Biomedical Engineering

performed at the MnF group

Faculty of Science and Technology

UNIVERSITY OF TWENTE.

July 22, 2021

L.G. van der Woerd
Student number: S2157179

Committee members
Prof.Dr.Ir. P. Jonkheijm
N.D. Debera
Prof.Dr. P.C.J.J. Passier

Abstract

This research was done to test if SLBs are a suitable surface for mimicking the micro-environment of cardiomyocytes. SLBs were functionalized with a cholesterol conjugated RGD peptide to see if this promotes similar adhesion as a vitronectin surface induces. Both the effect of the SLB on the cells as well as the effect of different culture media and the integrated peptide on the SLB were analysed. Both the cholesterol used for conjugating the RGD peptide as well as cholesterol soluted in CM medium was found to cause domain formation in the SLB. Integrating cholesterol into the SLB resulted in a decrease of its mobility.
Seeding cardiomyocytes on the SLBs caused them to be unstable. Influence of the functionalized surface on CMs seemed minimal compared to vitronectin.

Nederlands
In dit project is gekeken naar de mogelijkheid om lipide bilagen te gebruiken als ondergrond voor cardiomyocyten. De lipide bilaag zal bestaan uit DOPC en in een 96 well plaat worden gecreëerd. De ondergrond is gefunctionaliseerd met cholesterol-geconjugeerd RGD (chol-RGD). Zowel de invloed van de ondergrond op de cardiomyocyten als de invloed van de ondergrond op de cardiomyocyten is onderzocht.
Cholesterol zorgde voor aggegratie van de gebruikte fluorofoor in de lipide bilaag. De ondergrond bleek instabiel te worden wanneer hier cardiomyocyten op groeiden. Het experiment is herhaald met fibroblasten waarna de ondergrond niet instabiel werd. De invloed van de chol-RGD op de vasthechting van beide cell lijnen was verwaarloosbaar.

Acronyms

CMs Cardiomyocytes.

DLS dynamic light scattering.

ECM exctracellular matrix.

eGFP enhanced Green Fluorescent Protein.

FRAP fluorescence recovery after photobleaching.

hESCs human embryonic stem cells.

SLB supported lipid bilayer.

Contents

Chapter 1

Introduction

The cell membrane consists of a lipid bilayer in which different proteins and molecules are nestled.
Some of these proteins are cell receptors and have the purpose to communicate external events by cell signaling. Moreover, these receptors can be recognized by surrounding cells and perform the function of cell-cell communication.
Other proteins produced by the cells are excreted to the extracellular space and form the exctracellular matrix (ECM). The ECM is characteristic for each type of tissue and is mostly produced by fibroblasts, but tissue specific cells also play an important role in shaping their environment. Together, these elements form the characteristic micro-environment for each type of tissue. In the human heart, this micro-environment is formed by the cardiomyocytes themselves, cardiac fibroblasts, endothelial cells and the collagen-rich ECM.[1][2]

Cardiomyocytes (CMs) as well as cardiac fibroblasts are responsible for shaping the ECM of the heart, which is essential for optimal cell function.[3] Some of the ECM proteins contain an RGD peptide that integrins can bind to, this peptide has been shown to increase adhesion of cells.[4]
To study cell behaviour and their reaction to different factors, it is important to recreate the micro-environment these cells experience in the body.
In this research human embryonic stem cells (hESCs) derived cardiomyocytes' morphology and adhesion will be studied.[5] For this purpose, a cholesterol conjugated RGD peptide will be integrated in a supported lipid bilayer (SLB) to see if this will promote adhesion similarly to vitronectin, used as a positive control. A successful result can open up research for integrating other peptides into the SLB to create a more accurate representation of cells in vivo. This will make in vitro research more representative, and allows for determining the influence of specific components that make up the micro-environment in cell behaviour.

Chapter 2

Theory

2.1 Cells

2.1.1 Cardiomyocytes

The heart consists of two halves, composed out of two ventricles and two atria. Both have the ability to contract rhythmically to pump blood around the body. Part of the composition of the atria and ventricles are cardiomyocytes. These cells perform the bulk of contractility of the heart. For these cells to synchronously contract the heart they have to be very structured. The cells are cylindrical in shape and held together by a complex cytoskeleton which plays an important role in the interaction with the extracellular environment.
Three important cytoskeletal proteins converge at the place where integrins enter the cytosole, namely desmin and actinin (figure 2.1). The membrane of the cells is called the sarcolemma, a specialized structure consisting of a lipid bilayer. Its fundamental function is the blocking and passing of certain ions that control the action potential of the myocyte.[7]
The sarcolemma surrounds the sarcomeres. A sarcomere is composed of two main components, namely the contractile proteins and the cytoskeletal proteins. The contractile component consists of actin and myosin. Actin makes up the thin filaments, myosin the thick filament. Myosin has actin binding sites, each actin monomer has two myosin binding sites. Under the presence of ATP the interaction between these proteins leads to shortening of the sarcomere.

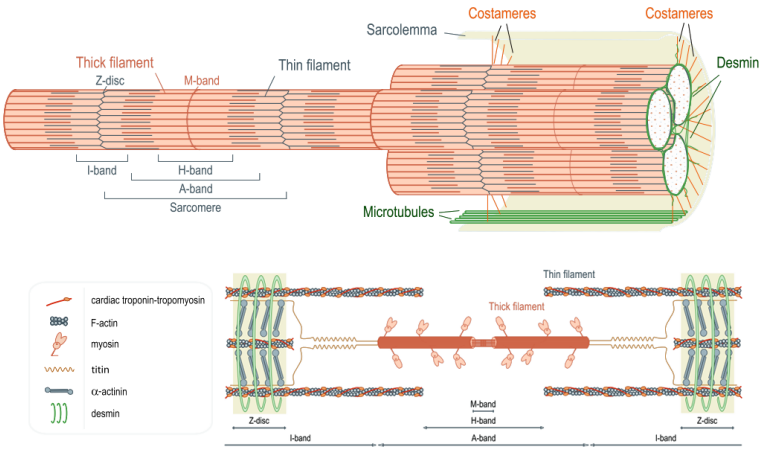

Figure 2.1: Schematic drawing of the anatomy of a cardiomyocyte showing how macroscopic structures are build up out of different proteins, specifically note the proteins making up the Z-disc. Image taken from [6].

The thin actin filaments are held together vertically with α-actinin and desmin, forming the Z-disc (figure 2.1).[6]

Cell-cell interaction

Individual cardiomyocytes are connected to each other via intercalated discs, a part of the sarcolemma that couples the cells together. The intercalated discs have an increased surface area due to their corrugated surface. This surface area is used to fit desmosomes, a protein structure that keeps the individual myocytes firmly together during contraction. Other structures found in the intercalated discs are gap junctions. These allow the flow of ions between adjacent cells, electrically coupling them. This makes it possible for the action potential to move through the heart, contracting the CMs in unison.
Important channels in the action potential of the cardiomyocyte are the K^+ and Na^+ channels. Hyperpolarization causes the K^+ channels to stop pumping potassium out of the cells, and let sodium flow into the cell causing the cell to become positively charged. When this hits a threshold Ca^{2+} channels open up resulting in contraction of the sarcomeres.[7]

2.1.2 DRRAGN Cardiomyocytes

For these studies a double reporter cell line is used. The cells are generated from a human embryonic stem cell line in which DNA coding for enhanced Green Fluorescent Protein (eGFP) was introduced in the NKX2.5 locus using homologous recombination.[8] This was turned into a double reporter line using CRISPR-Cas9 editing

to introduce expression for an mRubyII fluorescent α-actinin fusion protein. The resulting cells are called DRRAGN, standing for **D**ouble **R**eporter m**R**ubyII-**A**CTN2 **G**FP-**N**KX2.5.[5]
MRubyII excites at 559nm, while eGFP excites at 488nm.[9] This way Z-discs can be made visible, showing a striated pattern along the length of the cardiomyocytes. Expression of eGFP-NKX2.5 can be used to verify cells have in fact been correctly differentiated into cardiomyocytes, as it is a marker of the cardiomyocytes.[5]

2.2 SLBs

SLBs, or supported lipid bilayers, are a two dimensional surface consisting of lipid molecules held together by hydrophobic interactions.[10] The resulting surface is incredibly thin, as it is essentially two molecules thick. Depending on the lipids, this results in an average thicknesses of between 3.5 and 6 nm.[11] These layers can be used as a model of the cell membrane as proteins can be integrated in a similar way.[10] Hydrophobic molecules will nestle in between the layers, allowing translation and rotation within the layer when the used lipids are in their liquid phase, as opposed to the gel phase in which such movement is not freely possible.[12][13] This way the surface can be made to resemble the micro-environment cells experience in vivo. For example by introducing structural components produced by fibroblasts such as fibronectin or various types of collagen.[14]

2.2.1 SLB formation

SLBs can be created using various techniques, based on their application. For the coating of small particles the Langmuir–Blodgett/Langmuir–Schäfer method can be used. Coating of flat surfaces can be done in a multitude of ways. Vesicle fusion makes use of the hydrophilic properties of the surface. Spin-coating allows the formation of SLBs without the steps needed to create vesicles first. Then there is hydrodynamically driven vesicle fusion, which uses a hydrodynamic flow to induce SLB formation.
Other methods include vesicle fusion induced by α-helical peptides, and a combination of Langmuir–Blodgett and vesicle fusion shown in figure 2.2f.[12] These can be used dependent on their application.
In this experiment the glass bottom of a well plate will be used as the support for the lipid bilayer, for this the vesicle fusion method will be used to create the SLB.

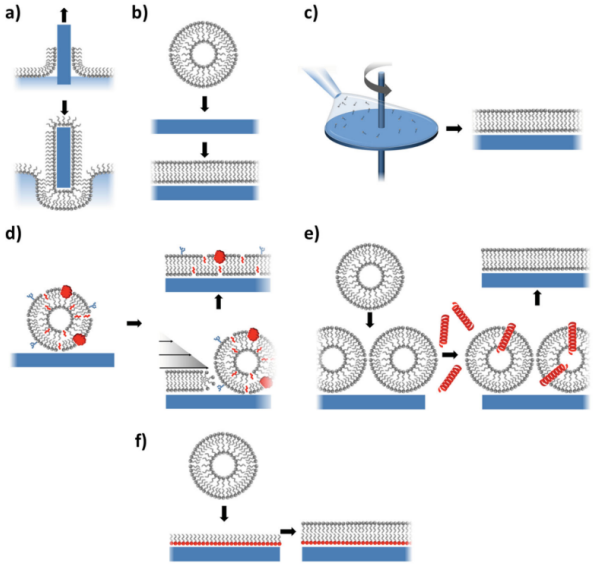

Figure 2.2: Common SLB formation techniques: a) Langmuir–Blodgett/Langmuir–Schäfer, b) vesicle fusion, c) spin-coating, d) hydrodynamically driven vesicle fusion, e) vesicle fusion induced by α-helical peptides, and f) a combination of Langmuir–Blodgett and vesicle fusion. Reprinted from [12].

To create SLBs by means of vesicle fusion, first unilamellar vesicles in the order of 100 nm need to be created. This consists of three different steps, the evaporation, rehydration, and the dispersion step.
First, the lipids are mixed and vacuum dried to create a lipid film at the wall of a glass vial. When this is rehydrated in milliQ, multilamellar lipid vesicles are formed. These will have to be turned into unilamellar vesicles. This can be done by sonification, extrusion or freeze-thawing.
Sonification makes use of sound waves to break particles, this however introduces heat into the mixture which could be unfavourable. It also lacks control over the vesicle size. Freeze-thawing repetitively will progressively fragment the multilamellar vesicles.[15] Though for this to work, electrolytes will have to be used in solution because it makes use of difference in osmotic pressure. This method results in vesicles smaller than 200nm, though not all at equal size.[16] Finally the multilamellar vesicles can also be extruded through a polycarbonate membrane with a well defined pore size to have more control over size distribution. This has to be done with the lipids in their liquid phase.

Formation of the SLB
To form an SLB on the substrate the created unilamellar vesicles will need to settle on the surface, rupture and form a single connected bilayer.[10] To make the glass surface more hydrophilic, first the surface needs to be hydroxylated. This can be done by incubating with NaOH.
Instability caused by osmotic pressure from the addition of a saline solution, like HEPES or DPBS, will make

it easier for the vesicles to rupture. This will turn into a chain reaction in which nearby vesicles rupture due to deformation stress. The formation of small patches leaves energetically unfavourable edges that in turn will induce further rupture of vesicles.[10]

2.2.2 Used lipids

For these experiments two different lipids will be used. The actual SLBs will be made up of DOPC. This lipid was used because of its availability at the time. It previously has also successfully been used with a similar purpose .[17] DOPC has a melting temperature of -20°C.[15]
Texas Red conjugated DHPE was used as a fluorescent marker, as it was available at the time as well as the similar length of its lipid tail to that of DOPC. TR-DHPE excites at 595 nm and emits at 615 nm. Both lipids are shown in figure 2.3.

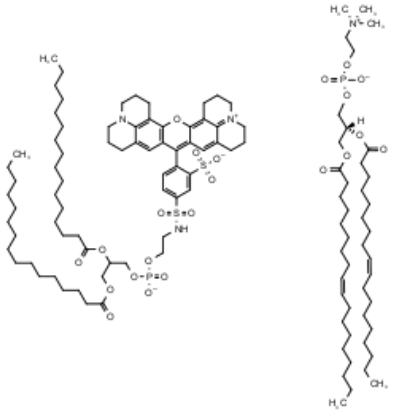

Figure 2.3: Lipids used in the making of SLBs. Left shows TR-DHPE, a fluorescent lipid. Right shows DOPC.

2.2.3 Variables in SLB formation

Important factors in the formation of SLBs are the solid support, charge of the solid support, as well as the charge of the individual lipids. The solid support needs to be hydrophilic to ensure the bilayer is formed at the surface. Calcium ions can help rupture the unilamillar vesicles and also help in the formation of the bilayer. The roughness of the support surface does not seem to influence SLB formation significantly.[10]

2.2.4 Cholesterol SLB interaction

Cholesterol is a natural occurring lipid that plays a role in the functioning of the cell membrane. It consists of hydrophobic steroid rings and a single polar group, giving it the ability to nestle into the lipid bilayer.[18] The polar group can be used to covalently bind other molecules, such as peptide sequences. For this project a KGSGRGDSG-peptide was bound to the cholesterol molecule using a succinate molecule as a linker connecting the N-terminal of the lysine to the polar group of the cholesterol molecule (figure 2.4).
Though calcium ions can help SLB formation, they are also strongly adsorbed by lipid bilayers.[19] These adsorbed calcium ions can in turn decrease the solubilization of cholesterol in a lipid bilayer.[20]

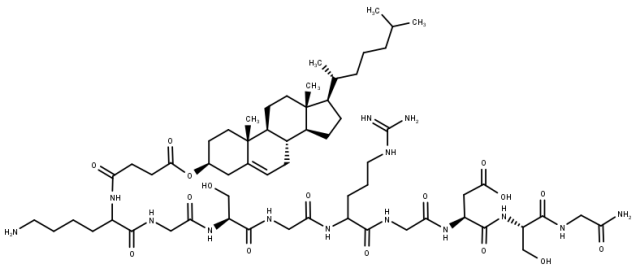

Figure 2.4: Molecular structure of the RGD motif-containing cholesterol structure (chol-RGD).

2.3 Vitronectin

Vitronectin is a serum protein with multiple functions. It plays a role in the immune system, helps with blood clotting, and can bind multiple proteins, but interestingly for our application is that it can also support cell adhesion. Vitronectin has been shown to support cell adhesion in vitro as well.[4] The RGD sequence in the protein is recognized by cells.[21] This RGD sequence is a tripeptide consisting of arginine, glycine and aspartate. It is recognized by the α and β subunits from the integrins in the cell to which it can bind. The β subunit of integrins contains a region for crosslinking with RGD peptides.[22]
Intracellular, this causes proteins such as talin and kindlin to bind to the integrin. After this, actin filaments are formed resulting in structural changes of the cell. These intricate connections with the ECM are called focal adhesions.[23]

2.4 Research aim

The aim of this research is to test if SLBs are a suitable surface for mimicking the micro-environment of cardiomyocytes. This will be done by integrating the chol-RGD into the surface and observing subsequent morphology changes of the cells.

Chapter 3

Methods

3.1 Surface preparation

3.1.1 SLBs for cell culture

A volume of 100 μl of 10 mg/ml DOPC in chloroform is transferred to a glass vial and dried using N_2 to create a lipid film. This was set to vacuum dry for at least one hour. Aluminium foil was used to prevent the incoming airflow from contaminating the film during repressurization. During desiccation, a black 96 well plate with glass bottom is hydroxilated with 100 μl/well of 1M NaOH and incubated for one hour. After incubation, wells are washed 10 times with milliQ. After desiccation the film is re-hydrated using 1ml of milliQ. This was then extruded 23 times through a membrane of 50 nm to create unilamellar vesicles. A volume of 0.8 ml of vesicle solution was collected. 3.2 ml of DPBS was added to create a 1:4 dilution. The DPBS destabilizes the vesicles for easier SLB formation. Following steps were performed sterile. Diluted SLBs were filtered, and subsequently added to the wells at 100 μl per well and incubated for 2 hours, then washed with DPBS 8 times by adding 100 μl, up and down pipetting and then removing a 100 μl to prevent air exposure of the SLB.
SLBs were stored in a fridge at 4°C.

3.1.2 SLBs for FRAP analysis

SLBs containing TR-DHPE were prepared to analyse the mobility of the surface using its fluorescence recovery after photobleaching. 99.65 μl of 10 mg/ml DOPC and 17.55 μl of 0.2mg/ml TR-DHPE is used. Blow drying, desiccation, rehydration, hydroxylation and extrusion steps are done similarly to the pure SLBs. After extrusion the vesicles are diluted 1:4 with PBS(regular). SLBs are then incubated at 100 μl per well for 2 hours, then washed with PBS 8 times by adding 100 μl, up and down pipetting and then removing 100 μl again to prevent air exposure of the SLB.
At 2 days, 1 day and 1 hour in advance, wells are washed 3 times with 100 μl medium to determine the effect of different media on the SLB. For this, DMEM Complete, cholesterol supplemented DMEM and CM medium were used.
Steps for creating fluorescent SLBs were repeated with DPBS instead of PBS to perform FRAP analysis on chol-RGD functionalized surfaces.

3.1.3 SLB functionalization

SLBs are functionlized with chol-RGD at 5 μM, 0.5 μM and 0.1 μM dissolved in DPBS. The wells are washed 5 times with 100 μl of the appropriate chol-RGD solution, then incubated for 2 hours at room temperature. After incubation wells are washed 5 times with DPBS.
Wells meant for cell culture were subsequently washed 2 times with applicable medium before starting cell seeding.

3.1.4 Vitronectin surface

300 μl of 5 $\mu g/ml$ vitronectin in DPBS is added to the wells and incubated for 1 hour in case of the CM plate. This resulted in a surface concentration of 4.8 $\mu g/cm^2$. For the fibroblast plate 100 μl of 1.7 $\mu g/ml$ vitronectin was used, because 300 μl was found to be a lot. The working surface concentration resulted in 0.5 $\mu g/cm^2$. Latter method was also used for the second CM experiment.

3.2 Cell culture

First CM seeding

Cells were thawed in a warm water bath, DMEM was added drop wise to prevent a calcium shock. Cells were then centrifuged and re-suspended in CM medium. Cells were counted with a Neubauer chamber at a dilution of 1:3 and directly used in cell culture. Cells were seeded at 125k cells/cm^2 and 250k cells/cm^2 resulting in a density of 40k and 80k cells/well respectively. Seeding was done in triplicate on five different surfaces. Vitronectin was used as the positive control, an SLB without functionalization as the negative control. SLBs were functionalized at 5 μM, 0.5 μM and 0.1 μM of chol-RGD solution.
Cells were incubated at 37°C with 5% CO_2.

Fibroblast seeding

NIH3T3 cells were used as a control. DMEM Complete was used as growth medium, consisting of DMEM supplemented wit 10% FBS, 1% Glutamine and 1% Penicillin and Streptomycin.
Cells were thawed, put into DMEM, then centrifuged and re-suspended in DMEM Complete. They were passaged in a T25 flask for one day at 37°C with 5% CO_2.
Cells were trypsinized for detachment, DMEM was added followed by centrifugation.
Cells were then re-suspended in DMEM Complete and counted using an EVE Automated cell counter at a dilution of 1:3. Seeding was done at a density of 10k and 5k cells/well. High density was seeded in 250μl of DMEM Complete, low density was seeded in 200μl DMEM Complete.

Second CM seeding

For the second experiment cells were seeded at a cell density of 64k/well. This time just the 0.1 μM chol-RGD concentration was used together with the positive and negative control. Experiment was conducted in triplicate.

3.2.1 CM medium

Used medium was made in house and kindly provided by the AST group. Medium was made up of 111 mM DMEM (Sigma), 0.5 mM Sodium Pyruvate (Thermo Fisher), 0,19 mM Sodium 3-hydroxybutyrate (Sigma), 0.5 mM L-Carnitine hydrochloride (Sigma), 1 mM Creatine monohydrate (Sigma), Taurine 5 mM (Sigma), Phenol Red 0.03 mM (Sigma), Trace elements A,B,C at 1 ml/L (Cellgro), CDLC, including cholesterol, at 10 ml/L (Thermo Fisher), GlutaMAX at 10 ml/L (Thermo Fisher), α-MTG 0.45 mM (Sigma), ITS-X 100 μl/L (Thermo Fisher), Ascorbic acid-2P at 50 $\mu g/ml$ (Sigma), Penicilin-Streptomycin at 5 ml/L (Thermo Fisher), $NaHCO_3$ at 3.7 gr/L. Cells were seeded with 200 μl medium, though RGD_1 (5 μM) were seeded with 300 μl.
Refreshment of the medium was performed by washing with medium 3 times to prevent air exposure of the SLB.

3.2.2 Data collection and analysis

DLS on vesicles was performed at a dilution of 1:20 of vesicles in milliQ to DPBS. Per condition 5 measurements were taken with a run time of 120s using a Nanotrac Wave W3043.
SLBs containing TR-DHPE were analysed using a confocal microscope (both a Zeiss LSM 880 and a Nikon A1 confocal microscope were used) at a wavelength of 561 nm.
FRAP analysis was performed at 561 nm laser with 100.0 power. Data points were collected every 1s until fluorescent signal seemed fully recovered, or for a maximum of 300s.
Brightfield images of cells were collected using a Olympus CKX41 microscope to confirm correct cell seeding and observe cell adhesion. Photos were taken using a modern mobile phone through the 10x ocular with a 4x, 10x and 20x objective.
EGFP fluorescence microscopy was done with a 460-490 nm exciter. MRubyII was captured with a 510-550 nm exciter. In both cases a 20x objective was used. Photos were taken with an Olympus DP70 camera mounted on an Olympus IX71 fluorescent microscope. Individual frames were contrast adjusted and then overlaid using ImageJ.

Methods described above for SLB formation, functionalization of these surfaces and vitronectin coating as well as seeding procedures are based on protocols optimized within the MnF group.

Chapter 4

Results

4.1 SLB

4.1.1 Formation of SLB

Extruded vesicles for SLB formation were analysed using dynamic light scattering (DLS). For each cell seeding a seperate batch of vesicles was created. A single batch of TR-DHPE vesicles was created for testing influence of CM medium. For testing DMEM Complete, cholesterol supplemented DMEM and functionalized SLBs, a different batch of TR-DHPE vesicles was created for a total of 5 batches. Peak size and peak width are represented in table 4.1. Size of vesicles does not change when stored for up to 2 weeks under N_2. Unilamellarity of the vesicles was not verified. This could have been done using NMR, but did not seem relevant as the process had already been validated.

Vesicles	Peak size (nm)	Peak width (nm)
CM seeding 1	67.2	34.9
CM medium	64.3	39.6
CM medium T+2 weeks	61.4	40.0
Fibroblast seeding	67.2	45.4
DMEM + chol-RGD	57.6	41.5
CM seeding 2	59.7	39.2

Table 4.1: Vesicle size before SLB formation.

Confocal fluorescence imaging was used to determine the formation and evenness of the SLBs. Images were taken at one day, two weeks and three weeks after formation to show the surfaces are stable over time, as is illustrated in figure 4.1. No increase in surface imperfections was observed over the span of three weeks with the plate stored at 4°C covered with DPBS.

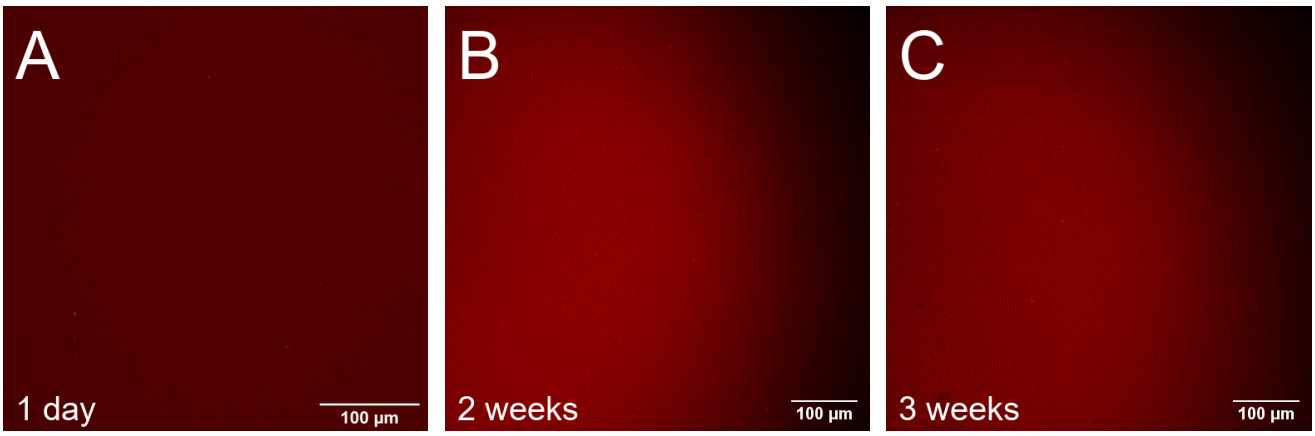

Figure 4.1: Confocal fluorescence imaging of SLBs at different time points. A was taken with a Zeiss LSM 880 confocal microscope, B and C were taken using a Nikon A1 confocal microscope. All images were taken with a 20x objective. A and C were created using the same vesicle batch, B was created with a different batch.

4.1.2 Functionilized SLBs

FRAP analysis was performed on functionalized SLBs. Characteristic diffusion time of SLBs functionalized at higher chol-RGD concentrations is larger, indicating a decrease in mobility. As is visible from figure 4.2C and D, more and larger clusters of TR-DHPE show up with a higher chol-RGD concentration.

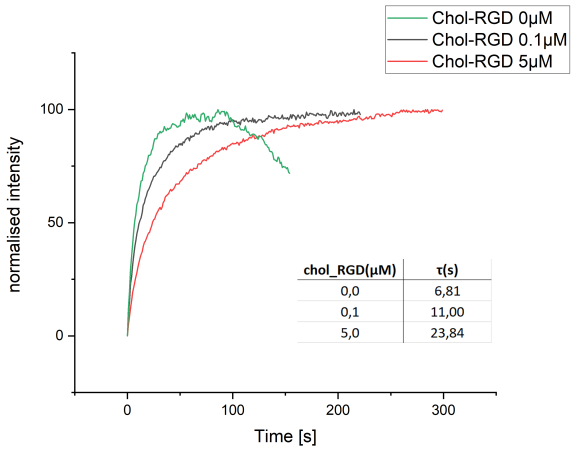

Figure 4.2: FRAP analysis of functionalized SLBs. Characteristic diffusion time is larger at higher chol-RGD concentrations.

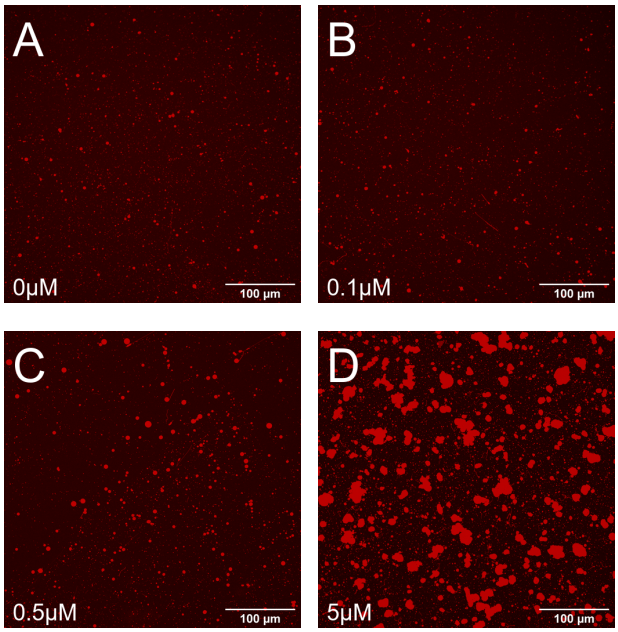

Figure 4.3: Confocal fluorescence images of SLBs functionalized with chol-RGD at different concentrations. Images were taken one day after functionalization. Aggregation of TR-DHPE is higher in conditions with higher chol-RGD concentrations, illustrated by C and D.

4.1.3 SLBs with medium

CM medium

SLBs were incubated with CM medium at different time points and analysed using FRAP.
FRAP analysis of SLBs incubated with CM medium showed that mobility of the SLBs was not affected by the incubation with CM medium. This is illustrated by the recovery lines of FRAP analysis plotted in figure 4.4. Nevertheless, fluorescence imaging shows an increase in aggregation of TR-DHPE, represented in figure 4.5C and D as an increase in red dots compared to figure 4.5A containing just DPBS.

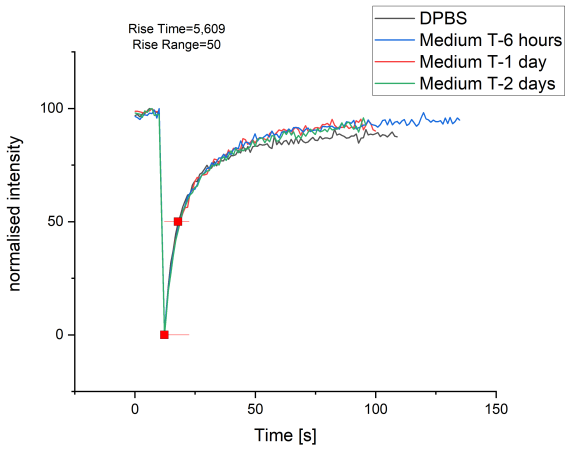

Figure 4.4: FRAP analysis of SLBs incubated with CM medium. Similar characteristic diffusion times show mobility is not affected by the medium.

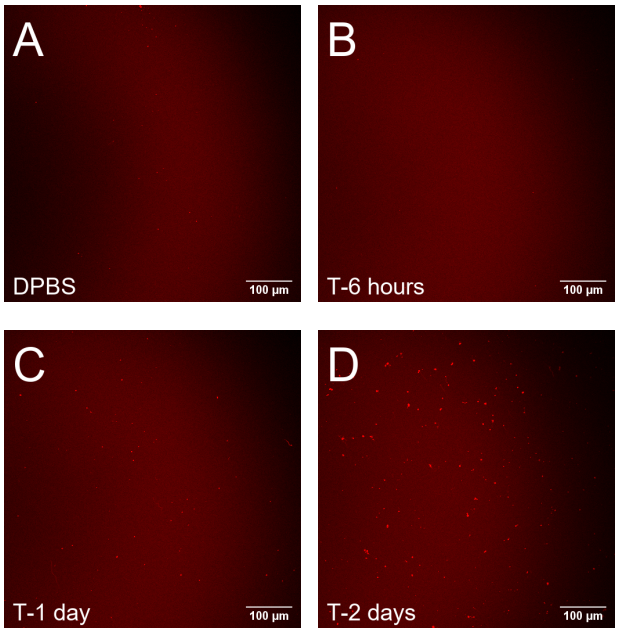

Figure 4.5: Fluorescence images of SLBs with CM medium added at different time points. Aggregation of TR-DHPE is more prominent in conditions C and D.

After about a day of incubation the effect of the medium on the SLB starts to appear. After initial imaging an additional washing step was performed to simulate the mechanical stress induced by a medium refresh on the SLB. Imaging done after this procedure does not seem to indicate rupture or increase of fouling of the surface.

DMEM Complete

The same experiment was performed with DMEM Complete. Earlier experiments showed DMEM had less impurities than just DPBS which might have been due to the extra washing because of the change of liquid. As a result the choice was made to create a condition in which the DPBS was washed as well. The condition without extra washing was still present. FRAP analysis was performed on these four conditions, shown in figure 4.6.
DPBS without extra washing does show a slower recovery. The three other conditions do have similar diffusion time, indicating again that the medium does not have a noticeable influence on the mobility of the SLB.
Figure 4.7 shows there is no increase in fouling, in contrary to the same experiment with CM medium. Of all four conditions the washed DPBS shows the most imperfections.

DMEM + Cholesterol

Adding cholesterol to DMEM shows a similar result to the CM medium experiment. A definite increase in imperfections is visible in figure 4.7F. Both E and F show more fouling than C and D respectively, which contain DMEM Complete.

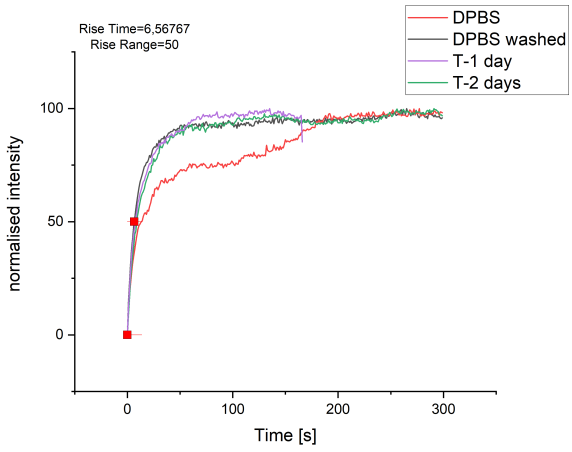

Figure 4.6: FRAP analysis of SLBs incubated with DMEM Complete. FRAP analysis was performed using both the regular DPBS as well as the DPBS with extra washing as a control. Similar characteristic diffusion times show mobility is not affected by the medium.

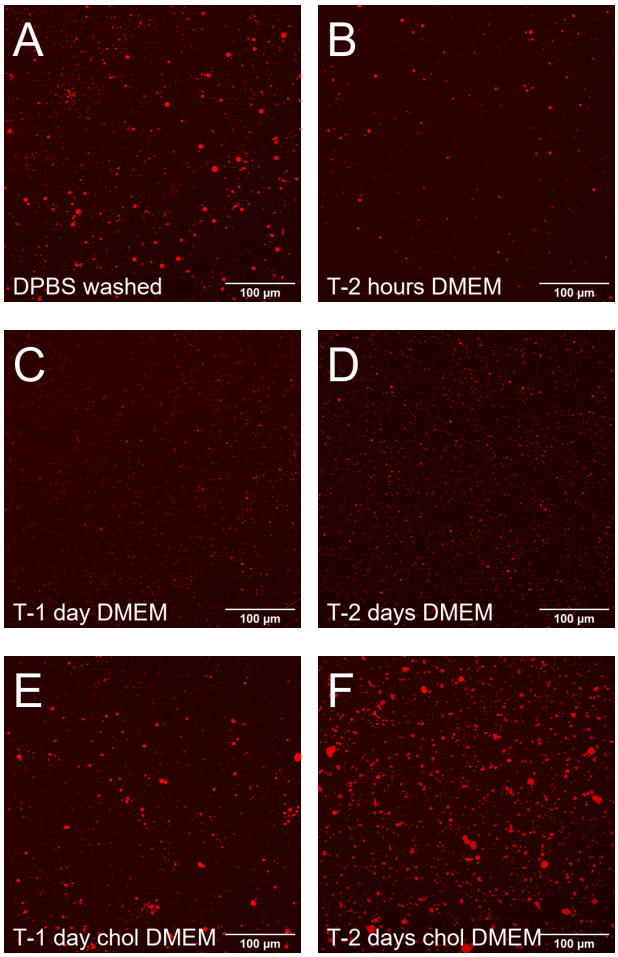

Figure 4.7: Fluorescence images of SLBs with DMEM Complete added at different time points (B, C and D), as well as cholesterol supplemented DMEM at different time points (E and F). There seems to be no difference in TR-DHPE aggregation over time in conditions containing DMEM Complete. DMEM with cholesterol however does show an increase in aggregation.

4.2 Cell culture

4.2.1 Cardiomyocytes seeding 1

CMs seeded on SLBs functionalized with 5 μM, 0.5 μM and 0.1 μM were observed at one day after seeding, shown in figure 4.9. The positive control with vitronectin coated wells show elongated cells. Also visible are filopodia like structures stretching out to nearby cells. 40k seeded wells shows this best due to a larger distance between individual cells.
Cells seeded on SLBs appear to be round. 80k density shows an increase in aggregated cells, this seems to slightly decrease with a higher chol-RGD concentration.
Performing a medium change by washing resulted in the SLBs to be destroyed indicated by the change in cell distribution (figure 4.8B). Cells seeded on vitronectin surfaces showed no change in cell distribution after medium change (figure 4.8A).

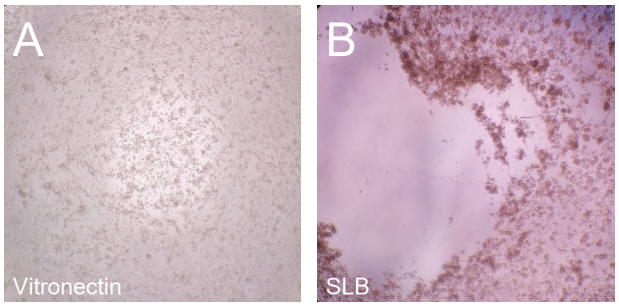

Figure 4.8: Brightfield imaging of cardiomyocytes at 1 day after seeding. A showing the vitronectin surface after refreshing medium. B showing how SLB surfaces looked after refreshing.

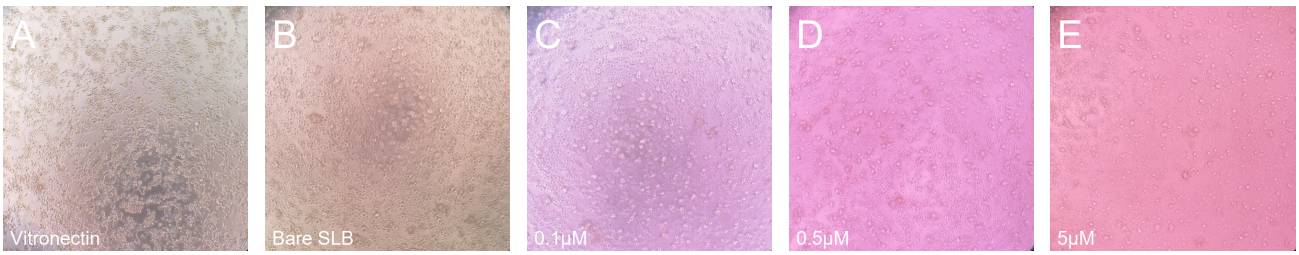

(a) Cells seeded at 40k/well

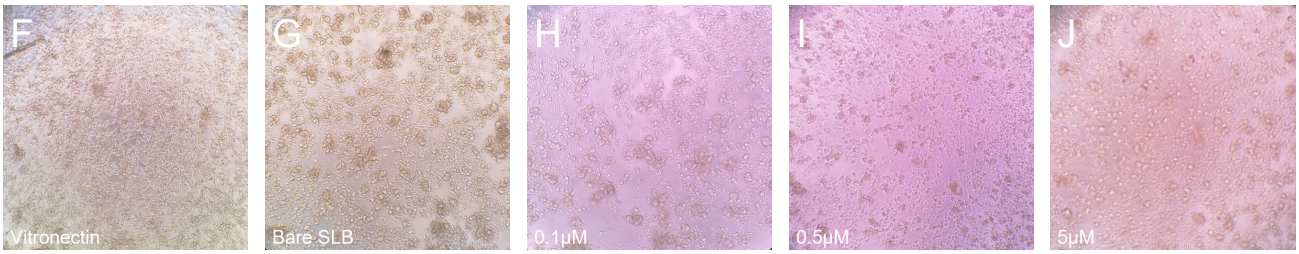

(b) Cells seeded at 80k/well

Figure 4.9: Brightfield imaging of cardiomyocytes at 1 day after seeding. A-E were seeded at 40k per well. F-J were seeded at 80k per well. Pictures were taken through a 10x ocular with a 4x objective.

4.2.2 Fibroblasts

Additional experiments were performed with fibroblasts to check if results were celltype dependent. The same concentrations of chol-RGD as for CM seeding 1 were used. Vitronectin was again used as the positive control, with a bare SLB as the negative control. Cells were seeded at a lower density of 10k/well because fibroblasts have a high proliferation rate, contrary to CMs.
All conditions show stretched cells indicating adhesion on all surfaces including the bare SLB. No change in cell distribution was observed after medium change. Low seeding density is left out because it did not show a different result, high cell seeding density is shown because it is more representative to the densities used for CM seeding.

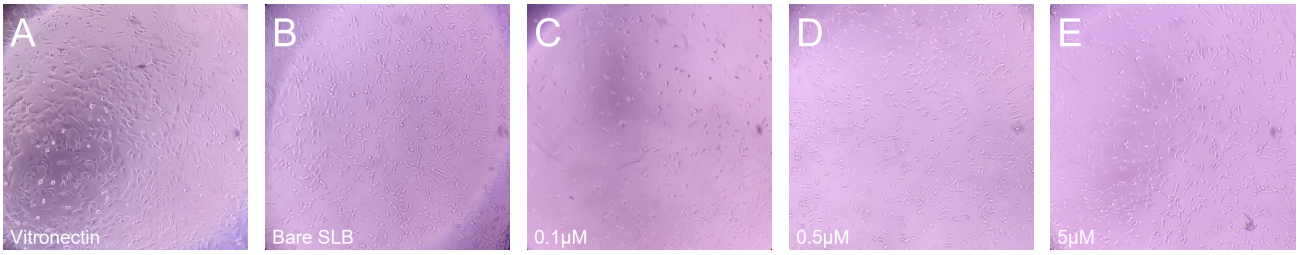

Figure 4.10: Brightfield imaging of fibroblasts 1 day after seeding. Cells were seeded at 10k per well. Images were taken through a 10x ocular with a 10x objective.

4.2.3 Cardiomyocytes seeding 2

For the second seeding of CMs the 5 μM, 0.5 μM chol-RGD condition were omitted due to their effect on the SLBs. Cells were seeded at a single density of 64k/well, as 80k looked to crowded, while the 40k density did not have enough cells to form a continuous monolayer. At one day after seeding vitronectin surface shows elongated cells. These elongated cells also appear to have more NKX2.5 expression than round cells indicating that they are in fact cardiomyocytes (figure 4.11A). Figure 4.11A also shows round cells without fluorescence indicating they might not be live cardiomyocytes. Both the bare SLB and 0.1 μM condition (figure 4.11H and I) show no adhesion or filopodia like structures. Here too structures showing no fluorescence are visible. Most of these structures are smaller than the cells that do fluoresce, as well as being circular in shape.

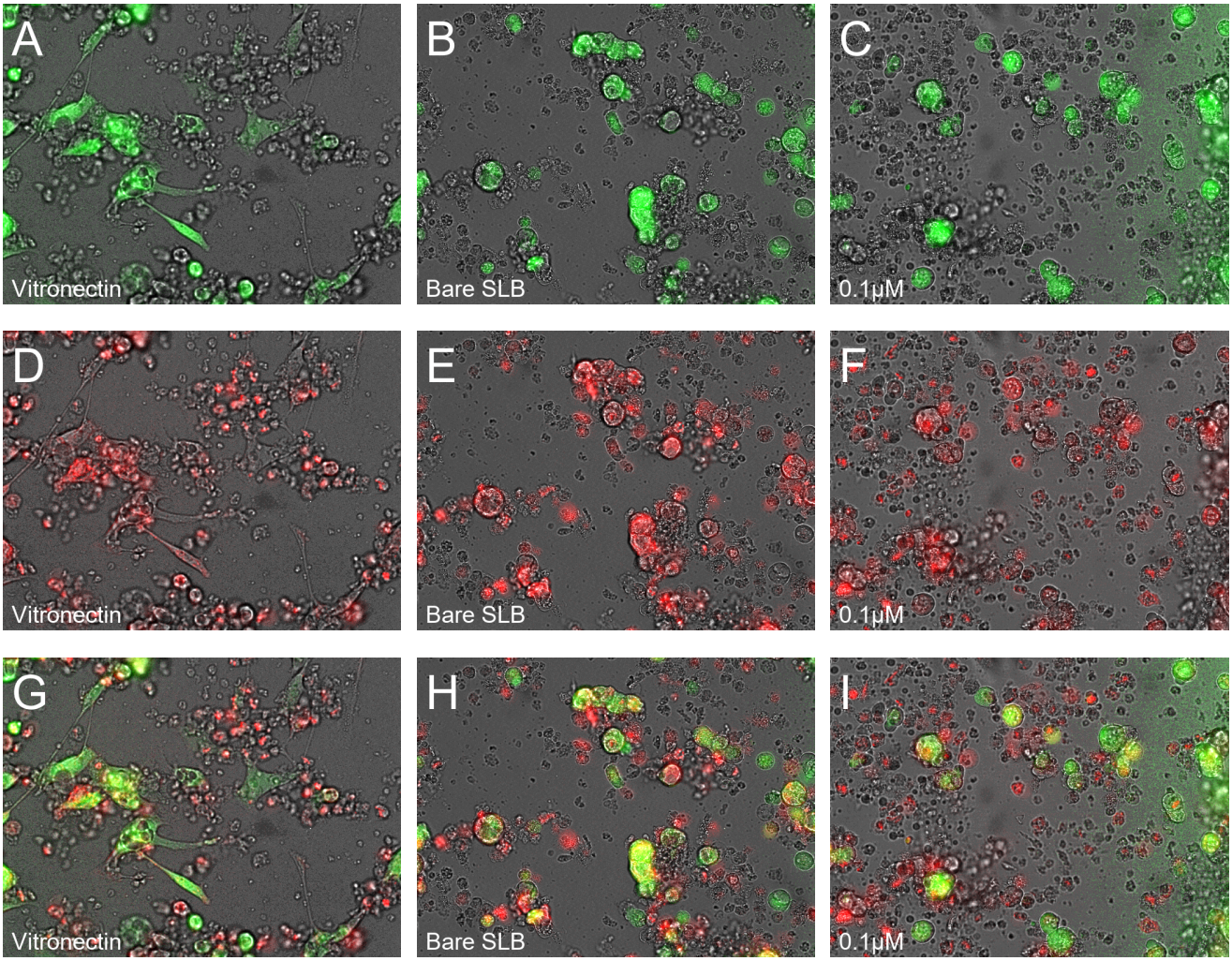

Figure 4.11: Fluorescence imaging of cardiomyocytes. Images were taken 1 day after seeding. Green coloration shows eGFP fluorescence which indicates NKX2.5 expression, red coloration shows mRUBYII fluorescence which indicates actinin. Seeding density is 64k cells/well. A 20x objective was used. A,D and G are control. B,E and H are negative control. C,F and I are functionalized SLBs. The top row shows NKX2.5 expression, the second row shows ACTN2 expression, the bottom row has both fluorescent signals overlaid.

Chapter 5

Discussion

SLB

Results from images of SLBs taken with a confocal microscope show that SLBs do not degrade over the span of three weeks. Storage of vesicles on the other hand does seem to degrade resulting SLBs, even though stored covered with N_2 at 4°C. SLBs created with two week old batches of vesicles showed more imperfections on the surface, so some experiments were repeated with fresh vesicles. This suggests it is better to create SLBs directly after extrusion of vesicles rather than storing vesicles for extended periods of time.
Surfaces that experienced extra washing steps due to adding of medium by washing showed less imperfections than the control. This resulted in the choice to add an extra control which included these extra washing steps as well. This control was cleaner and as a result had a higher mobility than the initial control (figure 4.6).
As is shown in figure 4.2 mobility decreases with chol-RGD concentrations. This might suggest that cholesterol decreases the mobility of SLBs. This can be unfavourable with the intent of mimicking the in vivo micro-environment.[24]
CM medium incubated SLBs however show no such decrease in mobility (figure 4.4) even though it has a cholesterol concentration of 5.7 μM, in line with the highest concentration chol-RGD used. Comparing this with FRAP analysis of cholesterol supplemented DMEM would have been interesting, but was not possible due to missing data. Lack in change of mobility from CM medium could be because the SLB is saturated by other molecules present in the medium, decreasing the uptake of cholesterol into the SLB.
Comparing confocal fluorescent imaging of DMEM Cmplete, cholesterol supplemented DMEM, CM medium and functionalized SLBs reveals that cholesterol probably plays a part in surface imperfections. Both the 2 day incubation of CM medium and cholesterol supplemented DMEM show more TR-DHPE aggregation. The same aggregation of TR-DHPE is illustrated by images taken of the 5 μM and 0.5 μM chol-RGD conditions (figure 4.3C and D), showing that this could be due to cholesterol. This is in line with what has previously been shown by Kocer, that addition of chol-RGD does lead to domain formation.[17]
This in turn could indicate that the chol-RGD is aggregating, resulting in an uneven peptide distribution over the surface.

Cell seeding

RGD-peptide was used to see if it was possible to promote similar adhesion of cells as vitronectin does. Results from the first cell seeding as well as the second CM seeding show adhesion of cells on SLBs does not compare to the positive control. All cells remain circular in shape without sign of elongation, suggesting chol-RGD functionalized SLBs do not promote cell adhesion.
This while the amount of RGD sequences/well is higher in wells containing chol-RGD than wells that were vitronectin coated. SLBs were exposed to 10, 50 and $500 \cdot 10^{-12}$ mol of chol-RGD, depending on the concentration. Vitronectin coated wells on the other hand were exposed to just $2.13 \cdot 10^{-12}$ mol. This could mean that uptake of chol-RGD into the SLB is very low.
Less cell aggregation in conditions with higher chol-RGD concentrations (figure 4.9b) on the other hand could indicate that cells do adhere more to the surface rather than to each other due to the functionalization. The bare SLB showing the most aggregation seems to confirm this (figure 4.9G).
As figure 4.8 shows, SLBs turned out not to be stable after incubation with cardiomyocytes, so the decision was made to perform the same experiment with fibroblasts.
Results form these experiment showed fibroblasts displayed no difference in adhesion on all SLB surfaces compared to the positive control. Surfaces remained intact after medium change.
This demonstrates SLB instability is specific to either cardiomyocytes or their medium. Although a bad batch of lipid vesicles cannot be ruled out.

Chapter 6

Conclusion

SLBs created with the method used in these experiment are stable over time when stored in a cold environment for up to three weeks. Vesicles are stable for about one week, stored under N_2 at 4°C, and should ideally be used for SLB formation immediately.
Introducing cholesterol into the SLB via either functionalization or it being dissolved in cell culture media increases domain formation and in case of functionalization also decreases the mobility of the SLB.
Washing of the SLB is an important step and should be done carefully and often.

Functionalized SLBs only have a very slight impact on adhesion of the cardiomyocytes. Combining this with the fact that the surfaces are not stable with these type of cells and their medium signifies SLBs are not a suitable surface for these types of analyses on cardiomyocytes.
Fibroblasts and their medium do not result in instability of the SLB. Though similarly to cardiomyocytes the functionalization of the surface has a negligible effect on adhesion.

Future work

As cholesterol is suspected as being the main culprit in the formation of domain separation, a different way of embedding peptides on SLBs could be tested.
Changing the surface in which the peptides are embedded could also mitigate the effect cholesterol has.
To further test the hypothesis that it is the cholesterol in the CM medium that causes the degradation of the SLB, an experiment with fibroblasts and cholesterol supplemented DMEM could be perforemed.

Bibliography

[1] Li Wang et al. "Single-cell reconstruction of the adult human heart during heart failure and recovery reveals the cellular landscape underlying cardiac function". In: *Nature Cell Biology* 22.1 (Jan. 2020), pp. 108–119. ISSN: 14764679. DOI: 10.1038/s41556-019-0446-7. URL: https://doi.org/10.1038/s41556-019-0446-7.

[2] Ana Catarina Silva et al. *Bearing My Heart: The Role of Extracellular Matrix on Cardiac Development, Homeostasis, and Injury Response*. Jan. 2021. DOI: 10.3389/fcell.2020.621644. URL: www.frontiersin.org.

[3] Edward C. Miner and Wayne L. Miller. *A look between the cardiomyocytes: The extracellular matrix in heart failure*. Jan. 2006. DOI: 10.4065/81.1.71.

[4] Alessandro Gandaglia et al. "Cardiomyocytes in vitro adhesion is actively influenced by biomimetic synthetic peptides for cardiac tissue engineering". In: *Tissue Engineering - Part A* 18.7-8 (Apr. 2012), pp. 725–736. ISSN: 1937335X. DOI: 10.1089/ten.tea.2011.0254. URL: /pmc/articles/PMC3313615/%20/pmc/articles/PMC3313615/?report=abstract%20https://www.ncbi.nlm.nih.gov/pmc/articles/PMC3313615/.

[5] Marcelo C. Ribeiro et al. "A cardiomyocyte show of force: A fluorescent alpha-actinin reporter line sheds light on human cardiomyocyte contractility versus substrate stiffness". In: *Journal of Molecular and Cellular Cardiology* 141 (Apr. 2020), pp. 54–64. ISSN: 10958584. DOI: 10.1016/j.yjmcc.2020.03.008. URL: https://doi.org/10.1016/j.yjmcc.2020.03.008.

[6] Vasco Sequeira et al. *The physiological role of cardiac cytoskeleton and its alterations in heart failure*. Feb. 2014. DOI: 10.1016/j.bbamem.2013.07.011.

[7] Elaine N. Marieb. *Human anatomy & physiology*. 10th. 2016, pp. 696–698.

[8] David A. Elliott et al. "NKX2-5 eGFP/w hESCs for isolation of human cardiac progenitors and cardiomyocytes". In: *Nature Methods* 8.12 (Dec. 2011), pp. 1037–1043. ISSN: 15487091. DOI: 10.1038/nmeth.1740.

[9] *FPbase :: The Fluorescent Protein Database*. URL: https://www.fpbase.org/.

[10] Ralf P. Richter, Rémi Bérat, and Alain R. Brisson. "Formation of solid-supported lipid bilayers: An integrated view". In: *Langmuir* 22.8 (2006), pp. 3497–3505. ISSN: 07437463. DOI: 10.1021/la052687c.

[11] Tzong Hsien Lee et al. "Effect of phosphatidylcholine bilayer thickness and molecular order on the binding of the antimicrobial peptide maculatin 1.1". In: *Biochimica et Biophysica Acta - Biomembranes* 1860.2 (Feb. 2018), pp. 300–309. ISSN: 18792642. DOI: 10.1016/j.bbamem.2017.10.007.

[12] Jasper van Weerd, Marcel Karperien, and Pascal Jonkheijm. "Supported Lipid Bilayers for the Generation of Dynamic Cell-Material Interfaces". In: *Advanced Healthcare Materials* 4.18 (Dec. 2015), pp. 2743–2779. ISSN: 21922640. DOI: 10.1002/adhm.201500398. URL: http://doi.wiley.com/10.1002/adhm.201500398.

[13] Luis A. Bagatolli and Roberto P. Stock. "Lipids, membranes, colloids and cells: A long view". In: *Biochimica et Biophysica Acta (BBA) - Biomembranes* 1863.10 (Oct. 2021), p. 183684. ISSN: 00052736. DOI: 10.1016/j.bbamem.2021.183684.

[14] Malina J. Ivey and Michelle D. Tallquist. *Defining the cardiac fibroblast*. 2016. DOI: 10.1253/circj.CJ-16-1003. URL: /pmc/articles/PMC5588900/%20/pmc/articles/PMC5588900/?report=abstract%20https://www.ncbi.nlm.nih.gov/pmc/articles/PMC5588900/.

[15] Wan-Chen Lin et al. *Supported Membrane Formation, Characterization, Functionalization, and Patterning for Application in Biological Science and Technology*. Vol. 2. 4. 2010, pp. 235–269. ISBN: 9780470559277. DOI: 10.1002/9780470559277.ch100131.

[16] Robert C Macdonald, Felecian D Jones, and Ruozi Qiu. *Biochi*
ic
a et Biophysica A£ta Fragmentation into small vesicles of dioleoylphosphatidylcholine bilayers during freezing and thawing. Tech. rep. 1994, pp. 362–370.

[17] Gülistan Koçer. *CELL-INSTRUCTIVE BIOINTERFACES WITH DYNAMIC COMPLEXITY*. ISBN: 9789036545204.

[18] Luciana de Oliveira Andrade. "Understanding the role of cholesterol in cellular biomechanics and regulation of vesicular trafficking: The power of imaging". In: *Biomedical Spectroscopy and Imaging* 5.s1 (Dec. 2016), S101–S117. ISSN: 22128794. DOI: 10.3233/bsi-160157.

[19] Adéla Melcrová et al. "The complex nature of calcium cation interactions with phospholipid bilayers". In: *Scientific Reports* 6 (Dec. 2016). ISSN: 20452322. DOI: 10.1038/srep38035. URL: /pmc/articles/PMC5131315/%20/pmc/articles/PMC5131315/?report=abstract%20https://www.ncbi.nlm.nih.gov/pmc/articles/PMC5131315/.

[20] Liliya Vinarova et al. "The mechanism of lowering cholesterol absorption by calcium studied by using an in vitro digestion model". In: *Food and Function* 7.1 (Jan. 2016), pp. 151–163. ISSN: 2042650X. DOI: 10.1039/c5fo00856e. URL: www.rsc.org/foodfunction.

[21] B FELDINGHABERMANN and D CHERESH. "Vitronectin and its receptors". In: *Current Opinion in Cell Biology* 5.5 (Oct. 1993), pp. 864–868. ISSN: 09550674. DOI: 10.1016/0955-0674(93)90036-P. URL: https://linkinghub.elsevier.com/retrieve/pii/095506749390036P.

[22] Stanley E. D'Souza, Mark H. Ginsberg, and Edward F. Plow. "Arginyl-glycyl-aspartic acid (RGD): a cell adhesion motif". In: *Trends in Biochemical Sciences* 16.C (1991), pp. 246–250. ISSN: 09680004. DOI: 10.1016/0968-0004(91)90096-E.

[23] Beatrice S. Ludwig et al. *Rgd-binding integrins revisited: How recently discovered functions and novel synthetic ligands (re-)shape an ever-evolving field*. Apr. 2021. DOI: 10.3390/cancers13071711. URL: https://www.mdpi.com/2072-6694/13/7/1711/htm%20https://www.mdpi.com/2072-6694/13/7/1711.

[24] P. Y. Chan et al. "Influence of receptor lateral mobility on adhesion strengthening between membranes containing LFA-3 and CD2". In: *Journal of Cell Biology* 115.1 (Oct. 1991), pp. 245–255. ISSN: 00219525. DOI: 10.1083/jcb.115.1.245. URL: http://rupress.org/jcb/article-pdf/115/1/245/1061883/245.pdf.